AGU PUBLICATIONS

Geophysical Research Letters

RESEARCH LETTER
10.1002/2016GL068409

Key Points:
- Length of Indian summer monsoon is an important metric
- Onset and demise date variations are important to Indian summer monsoon variability
- ENSO variations affect the length of the Indian summer monsoon

Supporting Information:
- Supporting Information S1

Correspondence to:
V. Misra,
vmisra@fsu.edu

Citation:
Noska, R., and V. Misra (2016), Characterizing the onset and demise of the Indian summer monsoon, *Geophys. Res. Lett.*, *43*, 4547–4554, doi:10.1002/2016GL068409.

Received 23 FEB 2016
Accepted 19 APR 2016
Accepted article online 20 APR 2016
Published online 7 MAY 2016

Characterizing the onset and demise of the Indian summer monsoon

Ryne Noska[1,2] and Vasubandhu Misra[1,2,3]

[1]Center for Ocean-Atmospheric Prediction Studies, Florida State University, Tallahassee, Florida, USA, [2]Department of Earth, Ocean and Atmospheric Science, Florida State University, Tallahassee, Florida, USA, [3]Florida Climate Institute, Florida State University, Tallahassee, Florida, USA

Abstract An objective index of the onset and demise of the Indian summer monsoon (ISM) is introduced. This index has the advantage of simplicity by using only one variable, which is the spatially averaged all-India rainfall, a reliably observed quantity for more than a century. The proposed onset index is shown to be insensitive to all historic false onsets. By definition, now the seasonal mean rainfall anomalies become a function of variations in onset and demise dates, rendering their monitoring to be very meaningful. This new index provides a comprehensive representation of the seasonal evolution of the ISM by capturing the corresponding changes in large-scale dynamic and thermodynamic variables. We also show that the interannual variability of the onset date of the ISM is associated with El Niño–Southern Oscillation (ENSO) with early (late) onsets preceded by cold (warm) ENSO.

1. Introduction

The arrival of the Indian summer monsoon (ISM) is clearly indicated by a dramatic increase in the mean daily rainfall from below 5 mm d^{-1} to over 15 mm d^{-1} in Kerala, the southwestern part of India [*Ananthakrishnan and Soman*, 1988; *Soman and Kumar*, 1993]. This onset, although regional in scale, is part of a larger progression of isochrones of the onset of the Asian monsoon stretching gradually from Southeast Asia across to northwest India and Pakistan [*Ramage*, 1971; *Janowiak and Xie*, 2003]. There are several other studies that have characterized the onset of the ISM with various dynamic [*Koteswaram*, 1958; *Ananthakrishnan et al.*, 1968; *Krishnamurti and Ramanathan*, 1982; *Wang et al.*, 2001, 2009] and thermodynamic [*Ananthakrishnan and Soman*, 1988; *Yanai et al.*, 1992; *Fasullo and Webster*, 2003; *Janowiak and Xie*, 2003] indices (Table S1 (Table (Figure) numbers starting with T (S) indicate they are in the supporting information); see supporting information for further discussion on comparison with these other indices). More recently, *Moron and Robertson* [2014] suggest that many of these yield similar onset dates, although their relationships with the local-scale onset of rains during the ISM vary.

There is a very rich history of several decades of research on the prediction and predictability of the onset of the ISM, which is summarized in *Wang et al.* [2009]. A sobering conclusion from that study is that despite so much research, there is still considerable subjectivity in the operational declaration of the onset of the ISM by the Indian Meteorological Department (IMD). Several studies have also shown from observations that the onset date of the ISM over Kerala has little bearing on the overall seasonal mean rainfall of the ISM [*Dhar et al.*, 1980; *Mooley and Parthasarthy*, 1984; *Mooley and Shukla*, 1987; *Misra and DiNapoli*, 2013]. However, the Hydrological Onset and Withdrawal Index (HOWI) based on vertically integrated moisture transport following *Fasullo and Webster* [2003] is promising as it simultaneously serves as a harbinger to the ensuing anomalous mean seasonal ISM rainfall. In this study we propose one such index for defining the onset and demise of the ISM but just based on precipitation.

2. Data and Methodology

We use the rainfall analysis based on rain gauges following *Pai et al.* [2014a, 2014b], which is available at a 0.25° grid spacing distributed across India from 1902 to 2005 at daily intervals. This data set has been extensively used for Indian monsoon studies. The proposed onset and demise index builds upon *Liebmann et al.* [2007] and an adaptation for the Asian Monsoon region in *Misra and DiNapoli* [2013]. We first define the all-India spatial average of rainfall as all-India rainfall (AIR). The onset and demise of the ISM is determined using AIR for a couple of reasons. Such a large-scale index is unlikely to have a false onset or demise by

transient weather systems that are unconnected to the seasonal evolution of the ISM. Typically, such false onsets are triggered by transient severe weather such as tropical depressions [*Krishnamurti et al*., 1981; *Flatau et al*., 2001], whose scales are much smaller than AIR. Also, seasonal AIR evolution and its variations are followed with great interest by a large community of people around the world and the current indices of the onset and demise, especially those based on onset over Kerala, have little bearing on overall seasonal ISM variations.

In order to objectively determine the onset and demise dates of the ISM for a particular year, the cumulative daily anomaly $C_m^{'}(i)$ of AIR for day *i* of year *m* is computed as

$$C_m^{'}(i) = \sum_{n=1}^{i} \left[D_m(n) - \overline{\overline{C}} \right], \tag{1}$$

where

$$\overline{\overline{C}} = \frac{1}{MN} \sum_{m=1}^{M} \sum_{n=1}^{N} D(m,n) \tag{2}$$

$D_m(n)$ is the daily AIR for day n of year m, and $\overline{\overline{C}}$ is the climatology of the annual mean of AIR over N (=365/366) days for *M* years. For illustration, we plot $D_{2000}(n)$ and $C_{2000}^{'}(i)$ in Figure S2. The onset of the ISM is defined as the day after $C_{2000}^{'}(i)$ reaches its absolute minimum, before the last three months of the year. Similarly, the demise of the ISM is defined as the day when $C_{2000}^{'}(i)$ reaches its absolute maximum after the onset date. These criteria give rise to objective characterization of onset and demise dates of the ISM. For example, the onset date of the ISM is 26 May and demise date is 28 September for the year 2000 (Figure S2). This index is henceforth the all-India rainfall onset and demise (AIROD). The time series of the AIROD and season length of the ISM are shown in Figure S3. None of these features of the ISM show a statistically significant linear trend, although significant variations at both high and low frequencies are apparent (Figure S3). Their means and standard deviations are given at the end of Table S2. A comparison of the mean and standard deviation of the AIR onset with those diagnosed from previous studies are shown in Table S3. The mean climatological onset date of AIR of 5 June coincides with the HOWI-based index [*Fasullo and Webster*, 2003], but the standard deviation is slightly higher in the former than the latter. All other indices vary in their climatological onset date by a few days. See supporting information for further discussion on this. The AIR onset precludes any false onsets caused by transient disturbances followed by several days of quiescent conditions. The readers are referred to the supporting information for further discussion on false onsets.

We also use the centennial atmospheric reanalysis from European Centre for Medium-Range Weather Forecasts called ERA-20C [*Poli et al*., 2013] to compare the seasonal evolution of some atmospheric variables (e.g., 850 hPa winds and 300 hPa temperature) with the AIROD. The ERA-20C is available daily at a 125 km grid interval (T159 spectral truncation), and its centennial time period overlaps with the gauge-based rainfall analysis data set. We also use the Climate Forecast System Reanalysis (CFSR [*Saha et al*., 2010]) for the daily evolution of some upper ocean (i.e., top 105 m) variables at a 0.5° grid spacing from 1979 to 2005; the HadISST1 data set [*Reynolds et al*., 2007] for global monthly averaged sea surface temperatures (SSTs) at a 1° grid spacing from 1902 to 2005; and National Center for Atmospheric Research's Niño 3.4 index [*Trenberth and Stepaniak*, 2000] at monthly interval from 1902 to 2005.

3. Results

3.1. Seasonal Evolution of the Indian Summer Monsoon

The composite rainfall prior to and after onset of the ISM is shown in Figure 1 to examine its climatological progression. It is apparent from Figure 1 that the northeastern part of India (commonly referred as the "seven sister states") receives heavy rainfall (~10–20 mm d^{-1}) more than a month prior to the onset, which is likely a result of the preceding East Asian monsoon. About a week prior to onset, rainfall over the northeastern region continues to be sustained while there is a moderate increase in rainfall (~5–10 mm d^{-1}) along the southwestern coast. On the day of the onset, rainfall in both of these regions greatly intensify (~20–30 mm d^{-1}) and parts of south-central and eastern India begin to receive light to moderate rainfall (~2–8 mm d^{-1}). Several days after onset, the rainfall over central India grows in magnitude (~10–20 mm d^{-1}) and progresses toward

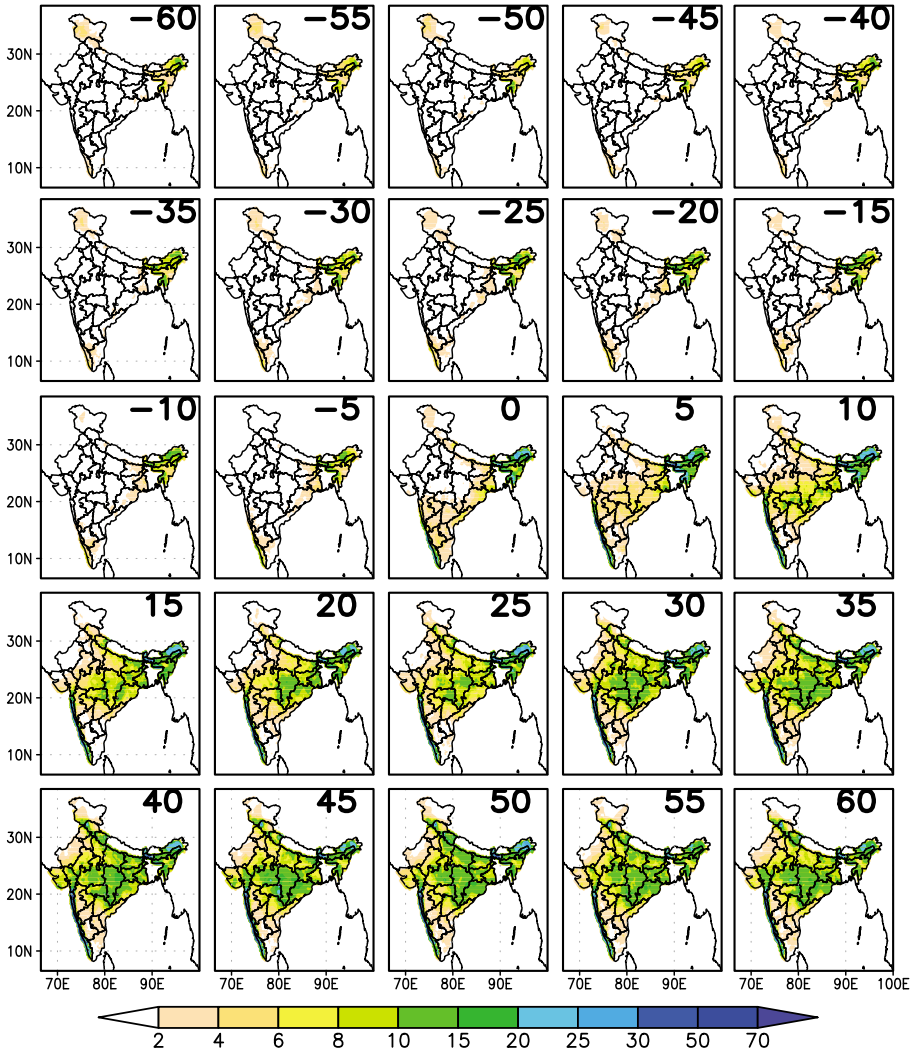

Figure 1. Seasonal evolution of the daily composite (averaged over 104 years from 1902 to 2005) of ISM rainfall prior to, at, and after the onset date at intervals of 5 days. Units are in mm d^{-1}.

the northwestern part of India, while the initial rain intensity in the southwestern coast and the northeastern region continues to be sustained (Figure 1).

A similar retreat of the rainfall centered on demise of the ISM can be ascertained from Figure S4. The withdrawal begins with the receding of rainfall from the northwest part of India. By the day of the demise, over 10 mm d^{-1} of rainfall is sustained only over the seven sister states, while the rest of India, excluding the northwest, exhibits a rain rate of about 2–6 mm d^{-1}. The continual withdrawal of the ISM steadily evolves into the advance of the northeast winter monsoon with rains in parts of southeastern India after the demise of the ISM (Figure S4).

Another robust seasonal feature of ISM evolution is the seasonal reversal of a rather strong meridional temperature gradient at around 300 hPa. *Yanai et al.* [1992] noted a reversal of the meridional temperature gradient between 5°N and 25°N, which is generally negative prior to onset and reverses to a positive value after the ISM is established. The AIROD captures this feature very well (Figure 2a), with the reversal of the temperature gradient (following the zero contour line) beginning in the eastern longitudes of the East Asian monsoon (east of 90°E) and steadily progressing westward. The temperature gradient reversal at around 60°E coincides with the day of onset of the ISM (zero lag on *y* axis) and slowly continues its journey westward after onset (Figure 2a). Conversely, the reversal of this meridional temperature gradient occurs earlier (later)

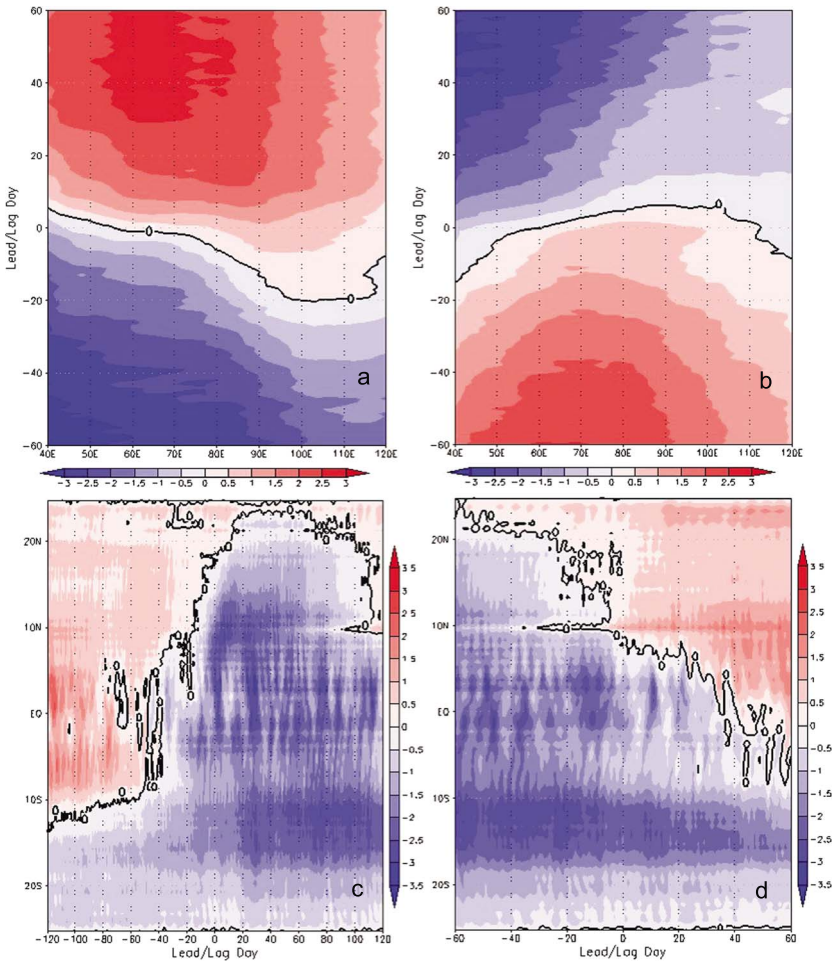

Figure 2. (a) The climatological daily zonal progression of the meridional temperature gradient between 5°N and 25°N at 300 hPa as a function of lead/lag time with respect to onset date of the ISM from 40°E to 120°E. Here negative (positive) values on the *y* axis refer to the meridional temperature gradient leading (lagging) the onset date. Units are in °C/1000 km. (b) Same as Figure 2a but centered on the demise date. (c) The climatological daily meridional progression of zonally averaged meridional ocean heat transport computed to a depth of 105 m (approximately mixed layer depth of the tropical Indian Ocean) from the Climate Forecast System Reanalysis (CFSR) [*Saha et al.*, 2010] as a function of lead/lag time with respect to the onset date of the ISM from 25°S to 25°N. Here negative (positive) values on the *x* axis refer to the meridional heat transport leading (lagging) the onset date. Units are in 0.1 PW. (d) Same as Figure 2c but centered on the demise date. The zero contour line is shown in black in Figures 2a–2d.

than the demise date of ISM west (east) of ~60°E (Figure 2b). However, it should be noted that some recent studies [e.g., *Boos and Kuang*, 2010, 2013] indicate that Tibetan Plateau serves to preserve the moist static energy of the monsoon by shielding it from the dry and cold extratropical air rather than serving to the evolution of the monsoon from its surface fluxes as an elevated heat source.

An additional feature that heralds the arrival of the ISM is the dramatic seasonal development of the low-level southwesterlies over the Indian Ocean, from which the monsoon derives its name, and the explosive growth of kinetic energy of these low-level winds [*Krishnamurti and Ramanathan*, 1982]. *Krishnamurti and Ramanathan* [1982] identify a region from 50°E to 70°E and from 4°S to 20°S as a domain of abrupt increase in zonal kinetic energy of 850 hPa winds for the year 1979. Figure S5 reveals a similar phenomenon for total kinetic energy of 850 hPa winds. Kinetic energy remains below 50 $m^2 s^{-2}$ from 50°E to 75°E and from 5°N to 20°N until less than a week before onset. It then rapidly triples to 150 $m^2 s^{-2}$ by onset of the ISM, and this generation of kinetic energy continues to grow to almost 300 $m^2 s^{-2}$ as the ISM progresses. Kinetic energy conversely decreases as the demise of the ISM approaches from about 50 $m^2 s^{-2}$ near 10°N almost 3 weeks

Table 1. Correlations Between Onset Date, Demise Date, Season Length, and Total Seasonal AIR Anomalies of the ISM[a]

	Onset Date	Demise Date	Season Length	Total Seasonal AIR
Onset date	**1**	−0.12	**−0.67**	**−0.43**
Demise date	−0.12	**1**	**0.82**	**0.61**
Season length	**−0.67**	**0.82**	**1**	**0.71**
Total seasonal AIR	**−0.43**	**0.61**	**0.71**	**1**

[a]Values significant at the 95% confidence interval are in bold.

before the demise to values below 25 $m^2 s^{-2}$ (Figure S6). By the day of the demise, only a small region of kinetic energy weaker than 50 $m^2 s^{-2}$ remains just south of the Indian peninsula (Figure S6).

An equally dramatic change in the direction of Ekman ocean heat transport is observed in the tropical Indian Ocean [*Wyrtki*, 1973; *Hastenrath and Lamb*, 1978; *Webster et al*., 1998; *Loschnigg and Webster*, 2000; *Chirokova and Webster*, 2006]. This results from the reversal of low-level atmospheric winds and their rapid growth in magnitude over the Indian Ocean as the ISM arrives. *Webster* [2000] shows that the seasonal reversal of the ocean heat transport in the Indian Ocean that effectively transports heat from the summer to the winter hemisphere nearly balances with the corresponding atmospheric heat transport from the winter to the summer hemisphere. The composite given in Figure 2c demonstrates that the equatorial Indian Ocean is dominated by upper ocean heat transport from the summer (northern) hemisphere to the winter (southern) hemisphere. About 120 days prior to the onset, southward meridional ocean heat transport is confined to regions below approximately 12°S, where a reversal to southward transport gradually advances further north to around 18°N by the time of onset (zero lag; Figure 2c). After onset, southward transport dominates the Indian Ocean from 25°S to 20°N. Meridional ocean heat transport then begins to gradually reverse from southward to northward about halfway through the monsoon season, and this reversal retreats southward to lower latitudes as the ISM progresses toward its demise (Figure 2d).

3.2. Interannual Variability of the Indian Summer Monsoon

A distinct advantage of the AIROD is its robust relationship with season length and total seasonal rainfall anomalies of the ISM (Tables 1 and S2). It should be noted that early (late) onset and demise dates are assigned negative (positive) anomalies. Also note that all correlations shown in this study are tested for significance at the 5% significance level with the bootstrap method [*Wilkes*, 2011]. Table 1 indicates statistically significant correlations of the onset date of the ISM with the length of the season. However, the correlations of the onset date variations are insignificant with the demise date variability of the ISM. It can therefore be discerned from Table 1 that early (late) onset of the ISM is associated with longer (shorter) length of the season and anomalously larger (smaller) accumulation of ISM rainfall seasonal anomalies. Similarly, Table 1 suggests that late (early) demise of the ISM is associated with long (short) season length of the ISM and large (small) accumulated seasonal rainfall anomaly of the ISM.

The variability of the AIROD offers a significant insight to the seasonal mean variations of the ISM. As mentioned before, the onset/demise of the ISM is characterized by large-scale changes including rain rate in several regions over India. Therefore, the seasonal rainfall anomalies have two sources of anomaly generation: variations in the length of the season and the daily rain rate. Both these factors are included in the accumulated seasonal rainfall anomalies of the ISM. As a result, onset date variation offers a robust estimate of the seasonal rainfall anomalies of the ISM (Figure 3a and Table 1). Figure 3a indicates that early (late) onset of the ISM is associated with widespread excess (deficit) of the seasonal rainfall anomalies from the southwestern coast to the northeastern region of India and including parts of central India. Similarly, we find that early (late) onset of the ISM is associated with a corresponding anomalous increase (decrease) of the positive temperature gradient at 300 hPa west of 90°E (Figure 3b). This figure shows that anomalous onset of the ISM is preceded and succeeded by about 20 days of anomalous meridional temperature gradient at 300 hPa west of 90°E. In other words, the anomalous onset date of the ISM identified through this methodology also represents the anomalous development of a land-temperature contrast in the domain.

The demise date variations in Figure S7 in contrast to Figure 3a show significant positive correlations with the ISM seasonal rainfall anomalies across India, including northwest India. In fact, these correlations are stronger than those displayed by the covariations with the onset date of the ISM (Table 1).

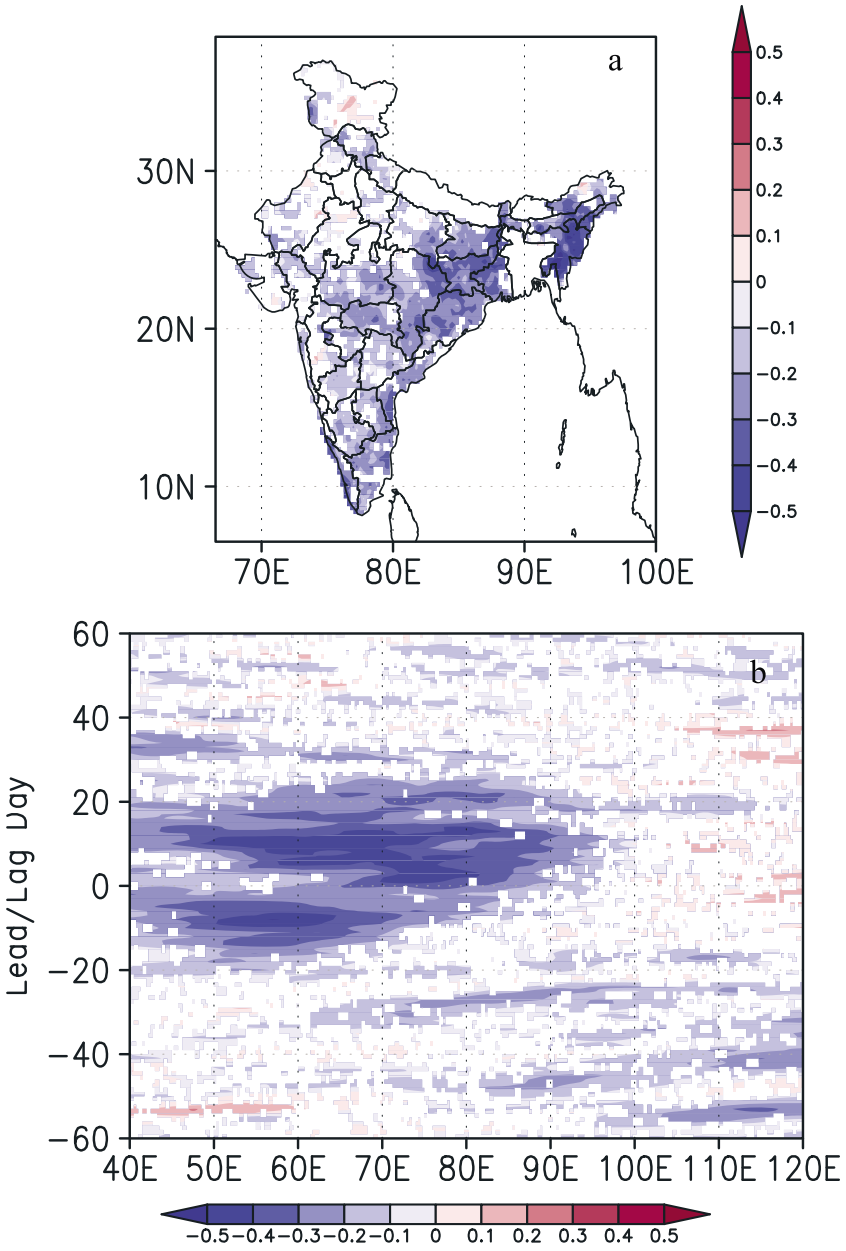

Figure 3. The correlation of onset date of the ISM with (a) following seasonal monsoon rainfall anomaly and (b) 300 hPa meridional temperature gradient from 5°N to 25°N at various lead/lag times. In Figure 3b, negative (positive) values on the *y* axis indicate that the temperature gradient is leading (lagging) the onset date. Only significant values at 95% confidence interval are shown.

Onset date variations of the ISM are also associated with the preceding December-January-February (DJF) SST anomalies in the eastern equatorial Pacific, reminiscent of the El Niño–Southern Oscillation (ENSO) variations (Figure 4). The correlations in Figure 4a suggest that warm (cold) ENSO is associated with following season's late (early) onset of the ISM. Figure 4b suggests that this relationship is strongest when Niño3.4 SST anomalies lead the onset date variations. But the correlations of the Niño3.4 SST anomalies with demise date are strongest when the latter leads. It may be noted that the correlations of June-July-August-September (JJAS) AIR anomalies and total seasonal AIR anomalies (includes seasonal length variations) with Niño3.4 SST anomalies are nearly the same. As a cautionary note, it may be mentioned that earlier studies have alluded to low-frequency variations of this teleconnection between ISM and ENSO [*Krishnakumar et al.*, 1999].

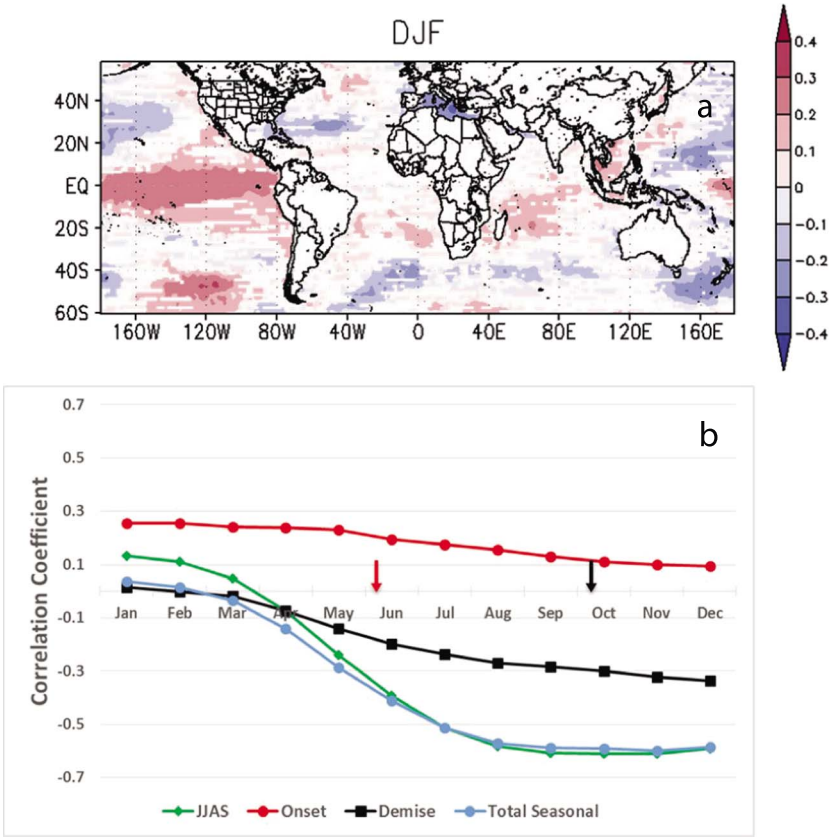

Figure 4. The correlation of the onset date of the ISM with (a) preceding December-January-February SST anomalies (HadISST1) [*Reynolds et al.*, 2007] and (b) Niño 3.4 SST anomalies [*Trenberth and Stepaniak*, 2001] at different lead/lag times (in months). In Figure 4b we also overlay the correlations of June-July-August-September (JJAS) ISM rainfall (green diamonds), onset (red circles) and demise (black squares) dates of the ISM, and total seasonal AIR (blue circles) with Niño3.4 SST anomalies. The red and black arrows in Figure 4b indicate the climatological onset and demise dates, respectively. Correlations prior to these dates would approximately correspond to SST leading the onset (demise) date of the AIR.

Figure S8 shows the comparison of total seasonal AIR with JJAS AIR. Following the IMD, anomalies of more than one standard deviation are considered anomalous. Both indices of the seasonal rainfall anomalies isolate anomalous dry and wet years for majority of the cases, although the magnitude of the anomalies differ (Figure S8). However, there are small but significant subset of years when they differ in defining anomalous ISM seasons. This stems from the fact that JJAS precludes anomalies defined by the increased or decreased length of the ISM. This is also expounded by the fact that the standard deviation of JJAS mean AIR (with climatological mean = 858.8 days) is 78.4 days while that of the total ISM season (with climatological mean = 887.4 days) is 107.1 days.

4. Conclusions

In this study we have proposed an index for the onset and demise of the ISM. This index has many merits. It is very simple, being based on a single variable, spatially averaged all-India rainfall, which has been reliably observed for over a century and allows those outside of the scientific community to perceive ISM variability more easily. Furthermore, the AIR-based onset and demise index is objective and avoids false onsets. It also has an advantageously close relationship with the seasonal rainfall anomaly. Therefore, the onset can be closely monitored to provide information regarding the likelihood of the development of an anomalous ISM season.

The index has been verified with the seasonal evolution of other dynamic and thermodynamic variables of the ISM and shown to be consistent with their evolution. The total seasonal rainfall anomaly, with its corresponding anomalous large-scale features, is also captured by the onset and demise index anomalies. Furthermore, all historic false onsets of the ISM are precluded by the onset index proposed here. In addition, ENSO variations also influence the onset date and demise date variations.

This index uses rainfall which is already observed across India, and minimal resources are therefore required to supplement existing methods for monitoring the onset of the ISM. It could be argued that one of the shortcomings of the proposed onset and demise index of the ISM is that it does not allude to local or regional onset and demise dates, which are equally important. We are currently working on ways to define the local onset and demise dates of the ISM that would contribute to this AIR-based onset and demise index.

Acknowledgments
We acknowledge the useful discussions and the programming support provided by Amit Bhardwaj and Akhilesh Mishra. The authors also gratefully acknowledge the financial support given by NOAA (NA12OAR4310078) and the Earth System Science Organization, Ministry of Earth Sciences, Government of India (grant MM/SERP/FSU/2014/SSC-02/002) to conduct this research under Monsoon Mission. We finally thank the Indian Meteorological Department for the availability of the daily rain analysis over India. The data used in this study are available upon request from the corresponding author.

References

Ananthakrishnan, R., and M. K. Soman (1988), The onset of south-west monsoon over Kerala: 1901–1980, *J. Climatol.*, *8*(3), 283–296, doi:10.1002/joc.3370080305.

Ananthakrishnan, R., V. Srinivasan, A. R. Ramakrishnan, and R. Jambunathan (1968), Synoptic features associated with onset of southwest monsoon over Kerala, Forecast Manual, Vol.IV-18.2, India Meteorological Department.

Boos, W. R., and Z. Kuang (2010), Dominant control of the South Asian monsoon by orographic insulation versus plateau heating, *Nature*, *463*, 218–222.

Boos, W. R., and Z. Kuang (2013), Sensitivity of the South Asian monsoon to elevated and non-elevated heating, *Sci. Rep.*, *3*, 1192, doi:10.1038/srep01192.

Chirokova, G., and P. J. Webster (2006), Interannual variability of Indian Ocean heat transport, *J. Clim.*, *19*, 1013–1031.

Dhar, O. N., P. R. Rakhecha, and B. N. Mandal (1980), Does the early or late onset of monsoon provide any clue to subsequent rainfall during the monsoon season, *Mon. Weather Rev.*, *108*, 1069–1072, doi:10.1175/1520-0493(1980)108<1069:DTEOLO>2.0.CO;2.

Fasullo, J., and P. J. Webster (2003), A hydrological definition of Indian monsoon onset and withdrawal, *J. Clim.*, *16*(19), 3200–3211, doi:10.1175/1520-0442(2003)016<3200a:AHDOIM>2.0.CO;2.

Flatau, M. K., P. J. Flatau, and D. Rudnick (2001), The dynamics of double monsoon onsets, *J. Clim.*, *14*(21), 4130–4146, doi:10.1175/1520-0442(2001)014<4130:TDODMO>2.0.CO;2.

Hastenrath, S., and P. Lamb (1978), On the dynamics and climatology of surface flow over the equatorial oceans, *Tellus*, *30*(5), 436–448, doi:10.1111/j.2153-3490.1978.tb00859.x.

Janowiak, J. E., and P. Xie (2003), A global-scale examination of monsoon-related precipitation, *J. Clim.*, *16*, 4121–4133.

Koteswaram, P. (1958), The easterly jet stream in the tropics, *Tellus*, *10*(1), 43–57.

Krishnakumar, K., B. Rajagopalan, and M. A. Cane (1999), On the weakening relationship between the Indian monsoon and ENSO, *Science*, *284*(5423), 2156–2159, doi:10.1126/science.284.5423.2156.

Krishnamurti, T. N., and Y. Ramanathan (1982), Sensitivity of the monsoon onset to differential heating, *J. Atmos. Sci.*, *39*(6), 1290–1306, doi:10.1175/1520-0469(1982)039<1290:SOTMOT>2.0.CO;2.

Krishnamurti, T. N., P. Ardanay, Y. Ramanathan, and R. Pasch (1981), On the onset vortex of the summer monsoon, *Mon. Weather Rev.*, *109*, 344–363, doi:10.1175/1520-0493(1981)109<0344:OTOVOT>2.0.CO;2.

Liebmann, B., S. J. Carmargo, A. Seth, J. A. Marengo, L. M. V. Carvalho, D. Allured, R. Fu, and C. S. Verara (2007), Onset and end of the rainy season in South America in observations and the ECHAM 4.5 atmospheric general circulation model, *J. Clim.*, *20*(10), 2037–2050, doi:10.1175/JCLI4122.1.

Loschnigg, J., and P. J. Webster (2000), A coupled ocean-atmosphere system of SST regulation for the Indian Ocean, *J. Clim.*, *13*(19), 3342–3360, doi:10.1175/1520-0442(2000)013<3342:ACOASO>2.0.CO;2.

Misra, V., and S. DiNapoli (2013), The variability of the southeast Asian summer monsoon, *Int. J. Climatol.*, *34*(3), 831–301, doi:10.1002/joc.3735.

Mooley, D. A., and B. Parthasarthy (1984), Fluctuations in all-India summer monsoon rainfall during 1871–1978, *Clim. Change*, *6*(3), 287–301, doi:10.1007/BF00142477.

Mooley, D. A., and J. Shukla (1987), Variability and forecasting of the summer monsoon rainfall over India, in *Monsoon Meteorology*, edited by C. P. Chang and T. N. Krishnamurti, pp. 26–59, Oxford Univ. Press, Oxford, U. K.

Moron, V., and A. W. Robertson (2014), Interannual variability of Indian summer monsoon rainfall onset date at local scale, *Int. J. Climatol.*, *34*(4), doi:10.1002/joc.3745.

Pai, D. S., L. Sridhar, M. Rajeevan, O. P. Sreejith, N. S. Satbhai, and B. Mukhopadhyay (2014a), Development of a new high spatial resolution (0.25°×0.25°) long period (1901–2010) daily gridded rainfall data set over India and its comparison with eisting data sets over the region, *Mausam*, *65*(1), 1–18.

Pai, D. S., L. Sridhar, M. R. Badwaik, and M. Rajeevan (2014b), Analysis of the daily rainfall events over India using a new long period (1901–2010) high resolution (0.25°×0.25°) gridded rainfall data set, *Clim. Dyn.*, *45*(3–4), 1–22, doi:10.1007/s00382-014-2307-1.

Poli, P., et al. (2013), The data assimilation system and initial performance evaluation of the ECMWF pilot reanalysis of the 20th-century assimilating surface observations only (ERA-20C), ERA Report Series 14. [Available from http://old.ecmwf.int/publications/library/ecpublications/_pdf/era/era_report_series/RS_14.pdf.]

Ramage, C. (1971), *Monsoon Meteorology*, *Int. Geophys. Ser.*, vol. 15, 296 pp., Academic Press, San Diego, Calif.

Reynolds, R. W., T. M. Smith, C. Liu, D. B. Chelton, K. S. Casey, and M. G. Schlax (2007), Daily high-resolution-blended analyses for sea surface temperature, *J. Clim.*, *20*(22), 5473–5496, doi:10.1175/2007JCLI1824.1.

Saha, S., et al. (2010), The NCEP Climate Forecast System Reanalysis, *Bull. Am. Meteorol. Soc.*, *91*(8), 1015–1057, doi:10.1175/2010BAMS3001.1.

Soman, M. K., and K. K. Kumar (1993), Space–time evolution of meteorological features associated with the onset of Indian summer monsoon, *Mon. Weather Rev.*, *121*(4), 1177–1194, doi:10.1175/1520-0493(1993)121<1177:STEOMF>2.0.CO;2.

Trenberth, K. E., and D. P. Stepaniak (2000), Indices of El Niño evolution, *J. Clim.*, *14*, 1697–1701.

Trenberth, K. E., and D. P. Stepaniak (2001), Indices of El Niño evolution, *J. Clim.*, *14*(8), 1697–1701, doi:10.1175/1520-0442(2001)014<1697:LIOENO>2.0.CO;2.

Wang, B., R. Wu, and K.-M. Lau (2001), Interannual variability of Asian summer monsoon: Contrasts between the Indian and western North Pacific–East Asian monsoons, *J. Clim.*, *14*(20), 4073–4090, doi:10.1175/1520-0442(2001)014<4073:IVOTAS>2.0.CO;2.

Wang, B., Q. Ding, and P. V. Joseph (2009), Objective definition of the Indian summer monsoon onset, *J. Clim.*, *22*(12), 3303–3316, doi:10.1175/2008JCLI2675.1.

Webster, P. J. (2000), The coupled monsoon system, in *The Asian Monsoon*, edited by B. Wang, Springer, New York.

Webster, P. J., V. O. Magana, T. N. Palmer, J. Shukla, R. A. Tomas, M. Yanai, and T. Yasunari (1998), Monsoons: Processes, predictability and the prospects for prediction, *J. Geophys. Res.*, *103*(C7), 14,451–14,510, doi:10.1029/97JC02719.

Wilkes, D. (2011), *Statistical Methods in the Atmospheric Sciences*, 2nd ed., 704 pp., Academic Press, Oxford, U. K.

Wyrtki, K. (1973), An equatorial jet in the Indian Ocean, *Science*, *181*(4096), 262–264.

Yanai, M., C. Li, and Z. Song (1992), Seasonal heating of the Tibetan Plateau and its effects on the evolution of the Asian summer monsoon, *J. Meteorol. Soc. Jpn.*, *70*(1), 319–351.